



**HAL**  
open science

## High-resolution $^{19}\text{F}$ and $^1\text{H}$ NMR of a vinylidene fluoride telomer

Philip Wormald, Bruno Ameduri, Robin Harris, P. Hazendonk

► **To cite this version:**

Philip Wormald, Bruno Ameduri, Robin Harris, P. Hazendonk. High-resolution  $^{19}\text{F}$  and  $^1\text{H}$  NMR of a vinylidene fluoride telomer. *Polymer*, 2008, 49, pp.3629-3638. <10.1016/j.polymer.2008.06.043>. <hal-00320274>

**HAL Id: hal-00320274**

**<https://hal.science/hal-00320274v1>**

Submitted on 11 Sep 2008

**HAL** is a multi-disciplinary open access archive for the deposit and dissemination of scientific research documents, whether they are published or not. The documents may come from teaching and research institutions in France or abroad, or from public or private research centers.

L'archive ouverte pluridisciplinaire **HAL**, est destinée au dépôt et à la diffusion de documents scientifiques de niveau recherche, publiés ou non, émanant des établissements d'enseignement et de recherche français ou étrangers, des laboratoires publics ou privés.



HAL Authorization

# High-resolution $^{19}\text{F}$ and $^1\text{H}$ NMR of a Vinylidene Fluoride Telomer

Philip Wormald<sup>1\*</sup>, Bruno Ameduri<sup>2</sup>, Paul Hazendonk<sup>3</sup> and Robin K. Harris<sup>4</sup>.

<sup>1</sup> School of Chemistry, University of St Andrews, Purdie Building, St Andrews KY16 9ST, UK.

<sup>2</sup> Laboratory of Macromolecular Chemistry, Ecole Nationale de Chimie de Montpellier, Unite Mixte Recherché, CNRS 5076, 8 rue de l'Ecole Normale, F 34296 Montpellier Cedex 5, France.

<sup>3</sup> Department of Chemistry and Biochemistry, 4401 University Drive, University of Lethbridge, Alberta, Canada T1K 3M4.

<sup>4</sup> Department of Chemistry, University Science Laboratories, South Road, Durham, DH1 3LE, UK

Keywords:  $^{19}\text{F}$  and  $^1\text{H}$  NMR; Vinylidenedifluoride; Telomer; Scalar coupling;

\*Corresponding author: Dr Philip Wormald, School of Chemistry, University of St Andrews, Purdie Building, St Andrews KY16 9ST, U.K.

Tel +44-(0)1334-463382; Fax +44-(0)1334-463808; email pw22@st-andrews.ac.uk

## Abstract

The reaction products of vinylidene fluoride (VDF) with methanol as a telogen have been analysed in the solution state by  $^1\text{H}$  and  $^{19}\text{F}$  nuclear magnetic resonance (NMR). High-resolution  $^{19}\text{F}$  and  $^1\text{H}$  NMR spectra were achieved using high-power  $^1\text{H}$  and  $^{19}\text{F}$  decoupling respectively, giving superior resolution and revealing previously unresolved signals of the vinylidene fluoride telomer (VDFT).  $^1\text{H}$  and  $^{19}\text{F}$  homo- and hetero-nuclear scalar coupling constants are presented and the spectra of functional groups and reverse units (including the identification of short-chain structures) are discussed. Furthermore, the application of  $^{19}\text{F}$  or  $^1\text{H}$  decoupling for the correct assessment of reverse-unit content and degree of polymerisation is demonstrated. This work highlights the need for high-resolution spectroscopy to determine both the chemical structure and composition of these important fluoropolymers.

## INTRODUCTION

The large chemical shift dispersion of fluorine nuclear magnetic resonance (NMR) led to some of the first spectra determining the composition and structure of synthetic fluoropolymers<sup>1-3</sup>. These first structures were deduced from <sup>19</sup>F NMR spectra without <sup>1</sup>H decoupling revealing the characteristic head-to-head (H-H), head-to-tail (H-T) and tail-to-tail (T-T) monomer sequences of poly(vinylidene fluoride) (PVDF), which are well known in the literature. The development of high-field magnets offer <sup>19</sup>F spectra of greater sensitivity, which, combined with developments in probe technology, make feasible the observation of <sup>1</sup>H and <sup>19</sup>F with <sup>19</sup>F and <sup>1</sup>H decoupling respectively. Thus, a great improvement in spectral resolution was achieved. However, many laboratories do not have this facility, partially due to cost, and many assignments are still made using spectra of lower resolution. The problems of resolution and subsequent signal assignment for fluorinated polymers is often further complicated because analyses are made on samples of raw synthetic samples, which contain a mixture of reaction products, i.e. with varying chain lengths and functional groups from which, reverse units and end chain groups are estimated. Such analyses are, also important for the understanding of the polymerisation reactions and thus for finding improved efficiencies for producing fluoropolymers. Separation procedures have substantial drawbacks and NMR is the only technique sufficiently powerful to determine structural details of the reaction products *in situ*.

Multinuclear correlation experiments have been implemented on samples related to PVDF, often to gain resolution for a specific group of signals<sup>4-6</sup>. The assignments are often deduced from spectra of model compounds or of samples obtained by various synthetic pathways<sup>7-10</sup>. <sup>1</sup>H and <sup>19</sup>F solution-state NMR spectroscopy has revealed the presence of -CH<sub>3</sub>, -CH<sub>2</sub>OH and -CF<sub>2</sub>H end groups<sup>11-13</sup> but poor resolution often inhibits the identification of signals associating them with the adjacent main-chain or other structures. Furthermore, without decoupling the overlap of signals is considerable due to the extent and magnitude of <sup>1</sup>H and <sup>19</sup>F homo and heteronuclear scalar couplings<sup>14</sup>. We are here concerned with relatively small PVDF samples, i.e. with vinylidene fluoride telomer (VDFT) products. No extensive investigation using one- and two-dimensional solution-state NMR experiments on such samples by observation of <sup>1</sup>H and <sup>19</sup>F resonances while decoupling <sup>19</sup>F and <sup>1</sup>H, respectively, appears to have been carried out previously.

Comparison of coupled and decoupled spectra enables the scalar coupling constants to be determined, leading to a more accurate structural evaluation. Typical (H,F) coupling constants found in the literature for PVDF main-chain  $\text{CF}_2\text{CH}_2$  groups are  ${}^3J_{\text{F,H}} \sim 16$  Hz, and  ${}^4J_{\text{H,H}} = 0 - 5$  Hz, while  ${}^4J_{\text{F,F}}$  is typically 10 Hz.<sup>15-17</sup> The reverse unit provides a well-documented feature in the spectra of VDF materials, yet  ${}^3J_{\text{F,F}}$  (0 - 5 Hz) and  ${}^3J_{\text{H,H}}$  (3 -12 Hz) are often not resolved and therefore only a limited number of values have been documented for such systems. Usually the  ${}^3J_{\text{F,H}}$  coupling constants involved in reverse units are also reported to be of the order of 16 Hz<sup>18</sup>. Further couplings of importance are those of the end-groups showing  ${}^2J_{\text{F,H}}$  (55.2 Hz) and  ${}^3J_{\text{H,H}}$  (4.4 Hz) for  $\text{H-CF}_2\text{-CH}_2\text{-}$ ,  ${}^3J_{\text{H,H}}$  (7.5 Hz) for  $\text{CH}_3\text{-CH}_2\text{-}$ , and  ${}^3J_{\text{F,H}}$  (19.3 Hz) for  $\text{CH}_3\text{-CF}_2\text{-}$ <sup>17</sup>. For the observation of small coupling constants the linewidth and resolution of the spectrum are obviously of great importance, which is probably the main reason why  ${}^3J_{\text{F,F}}$  and  ${}^4J_{\text{H,H}}$  coupling effects are seldom seen in spectra of high molecular weight PVDF polymers. The  ${}^nJ_{\text{F,F}}$  couplings do not follow the same general behaviour as  ${}^nJ_{\text{H,H}}$  couplings. It is possible for groups in straight-chain fluorinated compounds such as VDF to have vicinal  ${}^3J_{\text{F,F}}$  couplings near to zero, whereas  ${}^4J_{\text{F,F}}$  coupling constants can be quite large,  $\sim 10$  Hz<sup>19</sup>. This must be taken into consideration when assigning coupling constants and thereby determining the structure.  ${}^{19}\text{F}$  COSY spectra can often give more correlations than are typically found in a  ${}^1\text{H}$ -COSY spectrum. Whilst many examples of  ${}^1\text{H}/{}^{19}\text{F}$  heteronuclear correlation experiments have been published<sup>20, 21</sup>, few have been applied to polymeric fluorine systems and it is noted that  ${}^{19}\text{F}/{}^{19}\text{F}$  TOCSY experiments involve a difficulty in creating a spin-lock over the entire  ${}^{19}\text{F}$  chemical shift range<sup>22</sup>. A  ${}^{19}\text{F}$ -COSY spectrum has revealed unambiguously the pentad assignments in isoregic poly(vinyl fluoride)<sup>23</sup> and on aregic poly(vinylidene fluoride)<sup>24</sup>, such that the main regiosequence assignments out to the heptad level were verified. One major advantage of the 2D COSY experiment is that correlations are observable when coupling between multiplet systems are not resolved in 1D spectra. This is usually the case for polymers, where couplings as large as 7–10 Hz may not be resolved because of the 10 Hz linewidths. In our earlier work on PVDF<sup>25</sup> we showed that a 2D COSY spectrum revealed peaks at  $\sim -107$  ppm, which were assigned to possible CF sites at chain-branching positions, as these signals showed no off-diagonal cross peaks. The literature suggests assignments for some of these peaks to  $\text{CF}_2\text{-CH}_3$  end groups and offers chemical shift calculations to justify assignments of other peaks

in this region to chain branching<sup>26, 27</sup>. Any variations such as hydroxyl groups, defect units or modification of existing functionalities are of great importance, specifically for further chemical modification resulting in enhanced material properties for applications in, for example, modified membranes in polymer electrolyte fuel cells<sup>28, 29</sup>. In earlier work<sup>25</sup> we suggested an extended structure for the reverse units and CF<sub>2</sub> groups adjacent to them. However, the corresponding protons of the reverse units and end chains and any correlations of protons to the fluorine signals at ~ -106 and -108 ppm were not investigated. Recently, we studied the reaction products of VDFT by solid-state NMR<sup>30</sup> which revealed a great difference in the solid characteristics and macroscopic properties of VDFT compared to those found by our previous solid-state NMR studies on PVDF<sup>25, 31-33</sup>. Therefore, in this paper, we characterize VDFT by <sup>19</sup>F and <sup>1</sup>H solution-state NMR spectroscopy to evaluate, structure, defect-unit content, degree of polymerisation and the effect decoupling has on the analysis. Coupling constants are reported where possible, but this is greatly dependent upon linewidth and scalar coupling attenuation (*vide supra*) for <sup>3</sup>J<sub>F,H</sub>, <sup>3</sup>J<sub>F,F</sub> and <sup>4</sup>J<sub>F,F</sub>, including relevant <sup>1</sup>J<sub>H,H</sub> couplings<sup>14</sup>. Furthermore, assignments of minor peaks in the <sup>1</sup>H and <sup>19</sup>F spectra, including chain end-groups and short-chain VDFT fragments are offered. Any new information provided by these assignments could influence perceived synthetic reaction pathways as the proton and fluorine spectra are often employed to deduce reaction products and their intermediates<sup>34</sup>.

Geminal (F,F) coupling constants are large (ca. 200 Hz) and in principle can affect spectra. In most cases, the two fluorines of a CF<sub>2</sub> group and the two protons of a CH<sub>2</sub> group are chemically (but not magnetically) equivalent, and further considerations are required<sup>25</sup>. Thus, the nuclei of a main-chain CF<sub>2</sub>-CH<sub>2</sub> group will give an [AX]<sub>2</sub> contribution to the total spin system. However, the magnitude of <sup>2</sup>J<sub>FF</sub> will render the result indistinguishable from that of an A<sub>2</sub>X<sub>2</sub> system<sup>35</sup>. When the CF<sub>2</sub> fluorines are chemically non-equivalent, which only occurs when the group is adjacent to a chiral centre (e.g. at branching points), the situation could be more complicated, but even here such fluorines are, in practice, rendered effectively equivalent by the coupling. Of course, the full spin system of a VDFT is actually very complex.

## EXPERIMENTAL

The VDF telomer was prepared as described in the literature<sup>34</sup>. The solution-state spectra were recorded at 22 °C on a Bruker 500 MHz Avance spectrometer equipped with a QNP probe and operating at 499.78 MHz for <sup>1</sup>H and 470.21 MHz for <sup>19</sup>F. The solvent was dimethylsulfoxide-d<sub>6</sub> (DMSO-d<sub>6</sub>). <sup>19</sup>F chemical shifts were measured and are quoted relative to the signal for a replacement sample of CFCl<sub>3</sub> and <sup>1</sup>H shifts are relative to the signal for tetramethylsilane. The one-dimensional <sup>19</sup>F spectra were recorded with the following parameters: spectral width 28 kHz; data size 32 k; pulse delay 1 s; pulse duration (90°) 11.9 μs. The one-dimensional <sup>1</sup>H spectra had a 7 kHz spectral width, pulse delay of 1 s and pulse duration (90°) of 10.5 μs. Standard Bruker pulse sequences were used for <sup>1</sup>H and <sup>19</sup>F COSY and <sup>1</sup>H /<sup>19</sup>F HETCOR spectroscopy, with 20 kHz spectral widths along the t<sub>1</sub> and t<sub>2</sub> directions, a 256 ×4k data-point matrix for <sup>19</sup>F and a recycle delay of 3 s. For <sup>1</sup>H experiments, 4 kHz spectral widths in t<sub>1</sub> and t<sub>2</sub> and a 256 ×2 k data point matrix were used in the COSY experiments. Similar parameters were used in the HETCOR experiment.

Figure 2

## RESULTS AND DISCUSSION

### 1. Major signals in the <sup>1</sup>H and <sup>19</sup>F spectra of VDFT

Firstly, most of the major signals in the <sup>19</sup>F and <sup>1</sup>H spectra of VDFT, with and without decoupling, and their structural assignment by correlation spectroscopy will be discussed, since many of these signals are common to VDF-type structures and are well known<sup>17, 25, 36</sup>. Figure 1 shows the fluorine-coupled proton spectrum of VDFT with expansions (a, b, c and d). This spectrum involves both <sup>3</sup>J<sub>H,H</sub> and J<sub>F,H</sub> coupling patterns, as listed in Table 1 together with assignments, integrals and magnitudes of J<sub>F,H</sub> couplings. The peaks are denoted by Greek letters, and the assignments become clear when the splitting patterns are considered and the results of two-dimensional experiments evaluated. The fluorine-decoupled proton spectrum (Figure 2b) shows an increase in proton resolution, which allows a more accurate determination of chemical shifts and proton homonuclear coupling strengths (as given in Table 1 and quoted in the text below), and also identification of the heteronuclear <sup>3</sup>J<sub>F,H</sub> coupling constants by comparison with the fluorine-coupled proton spectra. The relative signal intensities, given in Table 1, were obtained by integration of the fluorine-decoupled spectrum only. The <sup>1</sup>H COSY (Figure 3 and Table 2) shows the proton-to-proton coupling,

Figure 1

Table 1

Figure 2

Figure 3

with signal assignments given in Table 1. Figures 4a and 4b show the  $^{19}\text{F}$  spectra (proton-coupled and proton-decoupled respectively).

Table 2

The one-dimensional spectra contain a number of signals that are well known in the literature. An intense quintet at 2.905 ppm ( $\phi$ ) (Figure 1) is identified as the main-chain protons in  $-\text{CF}_2-\text{CH}_2-\text{CF}_2-$  structures of the polymer backbone<sup>11-13</sup>. This signal is reduced to a broad singlet in the  $^{19}\text{F}$ -decoupled spectra (Figure 2), with no visible splitting, probably because the proton-proton coupling is smaller than the linewidth of  $\sim 10$  Hz. The corresponding fluorine signal of the main chain is seen at  $-91.897$  ppm (HT), table 3 and in figure 4a and 4b. Both of these signals show very similar relative integral values in both proton and fluorine spectra.

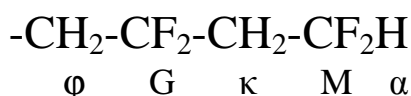
The decoupling does, however, reveal new low-intensity signals in both spectra for this region, which will be discussed later (see Section 3).

Figure 4

The proton resonance at 6.360 ppm ( $\alpha$ ) for  $-\text{CH}_2-\text{CF}_2\text{H}$  shows a characteristic triplet of triplets pattern (figure 1), with  $^2J_{\text{H,F}}$  (54.5 Hz) and  $^3J_{\text{H,H}}$  (4.5 Hz) coupling constants typical of end chains<sup>17</sup>. The signals  $\alpha$  and  $\kappa$  couple, as seen in the  $^1\text{H}$  COSY (Figure 3 and Table 2).

Figure 5

The signal  $\kappa$  is a quintet of doublets (Figure 1c), which becomes a doublet when fluorine-decoupled (Figure 2) and therefore has two  $\text{CF}_2$  groups adjacent to it, coupled by  $^3J_{\text{F,H}} \sim 16$  Hz, and one CH group. The signal M seen in the fluorine spectrum (Figure 4a, insert b) is assigned to the fluorine in the  $-\text{CH}_2-\text{CF}_2\text{H}$  end-group<sup>11, 12, 17</sup>. This signal shows  $^{19}\text{F}, ^1\text{H}$  coupling, causing a doublet splitting with  $^2J_{\text{F,H}} \sim 54.5$  Hz, and is split further into a triplet of triplets ( $^3J_{\text{F,H}}$  of 16.5 Hz and  $^4J_{\text{F,F}}$  of 6.0 Hz). The  $^{19}\text{F}/^1\text{H}$  HETCOR spectrum (Figure 5 and table 4) verifies the proton assignments of signals  $\alpha$  and  $\kappa$  to end-chain  $\text{CH}_2-\text{CF}_2\text{H}$  by demonstrating correlations to fluorine group M and (for  $\kappa$ ) to fluorine group G. Furthermore, the  $^{19}\text{F}$  COSY (Figure 6) shows that groups giving the signals M and G are near neighbours, proving that the end-group structure is  $\phi\text{-G-}\kappa\text{-M-}\alpha$  (Scheme 1).



Scheme 1

A complex triplet ( $\theta$ ) in Figure 1 at 2.267 ppm is in the region anticipated for the methylene groups of the reverse unit  $-\text{CH}_2-\text{CH}_2-\text{CF}_2-\text{CF}_2-$ <sup>25, 37</sup>. The  $^{19}\text{F}$ -decoupled spectrum of the same resonance (Figure 2) gives only a singlet, i.e. showing no (H,H) splitting. One would

expect to see a second-order  $[AB]_2$  pattern for these protons in the fluorine-decoupled spectrum, with additional splittings in the fluorine-coupled spectrum. The linewidth of the decoupled signal is  $\sim 6$  Hz. We assume the resonance arises from both methylene groups of the reverse units, the protons having almost identical chemical shifts so that the signals merge to form a singlet. A full assignment of the defect unit signals and those of the adjacent fluorine groups has been given<sup>24</sup> but is also described in this paper under Section 3. The less intense signals in the spectra present a greater challenge for interpretation. Many of these signals have been previously assigned by more tentative methods.

## 2. The occurrence of branching and/or end groups

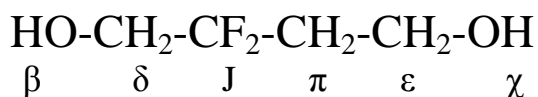
It has been suggested that the fluorine signals in the region between  $-106$  and  $-108$  ppm in the  $^{19}\text{F}$  spectrum of VDF materials (Figures 4a and 4b) derive from branching of the main chain<sup>26, 27</sup>, though no NMR spectra have convincingly confirmed all the signals in this region. We now attempt to clarify the nature of these signals and refer to the proton spectrum in Figure 1, which shows a triplet at 5.578 ( $\beta$ ) with a 6.5 Hz  $^3J_{\text{H,H}}$  coupling constant. This signal does not change with  $^{19}\text{F}$  decoupling (see Figures 1a and 1b) nor has it been reported in previous work. It is here tentatively assigned to a hydroxyl end-group on the basis of the chemical shift and coupling constant, which are similar to those of other such groups in VDFT<sup>34</sup>. A second triplet is seen at 4.751 ppm ( $\chi$ ) with a  $^3J_{\text{H,H}}$  coupling constant of 6.0 Hz, also assigned to a hydroxyl end group by reference to the literature<sup>34</sup>. Furthermore, signals between 3.650 and 3.570 ppm (Figure 1b) show a complex pattern, but can probably be interpreted as two triplets of doublets at 3.622 ppm ( $\delta$ ) and 3.600 ( $\epsilon$ ) for methylene protons of hydroxylated extremities  $-\text{CH}_2\text{-OH}$ . Figures 7a and 7b show the expanded region for both the  $^{19}\text{F}$ -coupled and -decoupled spectra of these two signals. In Figure 7b only the doublet is seen for the  $\delta$  signal, showing that the coupling is to the hydroxyl proton, whereas the signal for  $\epsilon$  remains unchanged. Hydroxyl structures have previously been suggested for these signals, but adjacent groups could not be determined with any great clarity<sup>34</sup>. However, from the  $^1\text{H}$  COSY spectrum (Figure 3 and Table 3), it is clear that the signal  $\epsilon$  couples to that labeled  $\pi$  at 2.138 ppm with  $\sim 6.5$  Hz and to  $\chi$  with  $\sim 5.5$  Hz, while  $\beta$  couples to  $\delta$  with  $\sim 6.5$  Hz. Furthermore both  $\pi$  and  $\delta$  have a  $^3J_{\text{F,H}}$  coupling of  $\sim 14.5$  Hz. The  $^1\text{H}/^{19}\text{F}$  HETCOR (Figure 5 and Table 4) shows that both  $\pi$  and  $\delta$  correlate

Figure 7

Table 3

Table 4

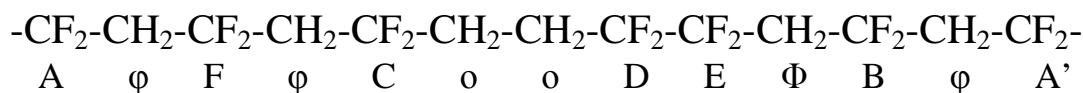
to the  $^{19}\text{F}$  signal J at  $-107$  ppm. This resonance is a quintet with a  $^3J_{\text{F,H}}$  (14.5 Hz) but is a singlet when decoupled (Figures 4a and 4b and Table 4). This strongly suggests that the fluorine signal at  $-107$  ppm (J) derives from a short-chain species and is not associated directly with end-chain groups of the VDF polymer backbone nor is it for a branch point; the structure is given in Scheme 2. The integrals of these signals also confirm the structure and verify it as a reaction by-product. Perhaps of greater interest is that these alcohol groups are not part of the major polymer fragment, and thus do not fulfil a major purpose of providing functionality for further chemical modification of the main polymer.



Scheme 2

### 3. The structure of the defect units.

There are several signals in the fluorine-decoupled proton spectrum (Figure 2) at similar chemical shifts to the main-chain signal at 2.905 ppm ( $\phi$ ); these are at 3.072 ( $\phi$ ), 3.012 ( $\gamma$ ), 2.997 ( $\eta$ ), 2.963 ( $\iota$ ), 2.837 ( $\omega$ ) and 2.792 ( $\omega$ ) ppm. The fine structure of these individual signals is difficult to interpret because of signal overlap. All of them have similar linewidths ( $\sim 6$  Hz) to that of the main-chain signal, and therefore no  $^4J_{\text{H,H}}$  coupling is seen. However, we do suggest they are probably from  $-\text{CH}_2-\text{CF}_2-\text{CH}_2$ -main-chain structure types, apart from the signal  $\phi$ , which correlates in the  $^{19}\text{F}/^1\text{H}$  HETCOR spectrum with resonance E of the  $\text{CF}_2$  group in the defect unit (Figure 5). The reverse unit  $\text{CH}_2$  signal ( $\circ$ ) at 2.267 ppm correlates to the fluorine signals D and C, seen in the same spectrum; therefore, C and D must be adjacent to the defect protons. The  $\text{CF}_2$  reverse groups D and E couple, as shown in Figure 6 (in spite of the lack of observable splittings in their spectra), and the signal  $\phi$  couples only to E (Figure 5), so  $\phi$  is adjacent to a reverse unit. Other groups in close proximity to these signals can also be assigned, since E couples to B and B to A'. Proton signals  $\phi$  and  $\phi$  both couple to resonance B. Furthermore, only D and C couple to signal  $\circ$ , F couples to both C and A but C and A do not couple, F, and all couple to the main-chain proton signal  $\phi$  (see Figure 5 and Table 4) giving assignments for the fluorine and proton signals of the defect unit with their adjacent groups (Scheme 3).



Scheme 3

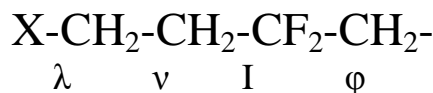
Figure 8

Moreover, the defect-unit signals in the expanded fluorine spectrum (Figures 8a and 8b) show that the linewidths of the proton-coupled signals are  $\sim 50$  Hz (E) and  $\sim 45$  Hz (D). By reference to Scheme 3 and literature values<sup>19</sup>, the signal E should be coupled by  ${}^4\text{J}_{\text{F,F}}$  ( $\sim 10$  Hz) from signal B and  ${}^3\text{J}_{\text{F,F}}$  (probably negligibly small) from D, but also  ${}^3\text{J}_{\text{F,H}}$  ( $\sim 16$  Hz) and  ${}^4\text{J}_{\text{F,H}}$  ( $\sim 5$  Hz) from  $\phi$  and o respectively. In the case of signal D, its largest splitting contribution would come from  ${}^3\text{J}_{\text{F,H}}$  ( $\sim 16$  Hz) since literature values predict a  ${}^3\text{J}_{\text{F,F}}$  of  $\sim 0$  Hz. Both signals have widths which are reduced by one third to  $\sim 33.0$  Hz (E) and  $\sim 16$  Hz (D) when proton decoupled. Proton decoupling seems, therefore, to be more effective on D than E. As discussed in the introduction,  ${}^3\text{J}_{\text{F,H}}$  and  ${}^4\text{J}_{\text{F,F}}$  should normally provide the strongest coupling in VDFT<sup>19</sup>; the broad signal for E reflects this. It is, however, possible to distinguish a triplet in signal D with a 14.0 Hz coupling, which must be to its nearest neighbour E, as D does not correlate to C in  ${}^{19}\text{F}$  COSY (Figure 6) (i.e., it shows no  ${}^5\text{J}$  coupling and no through-space coupling to C - often seen in COSY for other  $\text{CF}_2$  groups<sup>38</sup> as noted in the introduction). This would mean that the reverse unit  ${}^3\text{J}_{\text{FF}}$  coupling has a significant magnitude, in contrast to published values of near zero for straight-chain perfluorinated molecules.<sup>19</sup>

#### 4. Assignments of the various end groups and chain substructures.

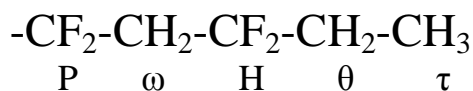
A proton singlet at 1.252 ppm ( $\sigma$ ) (Figures 1 and 2) is assigned to the methyl groups of the *tert*-butyl alcohol  $(\text{CH}_3)_3\text{-C-O-H}$  produced from the radical initiator di-*tert*-butyl peroxide  $((\text{CH}_3)_3\text{-C-O})_2$ , as noted in the literature<sup>34</sup>. The corresponding OH hydrogen in *tert*-butyl alcohol possibly exchanges with adventitious water to give the signal at 3.348 ppm. However, an alternative assignment is to a  $(\text{CH}_3)_3\text{-C-O-CH}_3$  structure containing the signal  $\mu$  at 2.653 ppm, which is a quartet and the only other signal of the same intensity as  $\sigma$ . Protons  $\lambda$ , giving a triplet at 2.720 ppm with  ${}^3\text{J}_{\text{H,H}}$  (7.5 Hz) and  $\nu$ , showing a triplet of triplets at 2.358 ppm with  ${}^3\text{J}_{\text{H,H}}$  (7.5 Hz) and  ${}^3\text{J}_{\text{F,H}}$  (16.5 Hz), correlate in the  ${}^1\text{H}$  COSY (Figure 3). Only the proton signal  $\nu$  correlates to the fluorine signal I at  $-95.568$  ppm, as

seen in the  $^{19}\text{F}/^1\text{H}$  HETCOR spectrum (Figure 5 and Table 4). As the signal  $\lambda$  is not affected by  $^{19}\text{F}$  decoupling nor is it adjacent to any fluorine group, its chemical shift would imply that an electronegative group is adjacent to it, possibly  $(\text{CH}_3)_3\text{-C-O-}$ , but this is speculative as the integrals do not verify this. Scheme 4.



Scheme 4

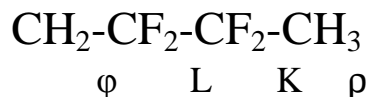
In Figure 1, a triplet of quartets is seen at 1.961 ppm ( $\theta$ ), showing both  $^3\text{J}_{\text{H,H}}$  (7.5 Hz) and  $^3\text{J}_{\text{F,H}}$  (16.5 Hz) coupling. The proton coupling magnitude and the intensity of this signal correspond to those for the triplet at 0.967 ppm ( $\tau$ ). These signals also show mutual coupling in the  $^1\text{H}$  COSY (Figure 3), but only the signal  $\theta$  couples to a  $\text{CF}_2$  group (H) at  $-95.330$  ppm, which also couples to the main-chain protons  $\phi$  as seen in the  $^{19}\text{F}/^1\text{H}$  HETCOR spectrum (Figure 5). Further coupling with agreeable integrals are that of H to P. On the basis of such assignments and integrals, these signals represent an end group, as shown in Scheme 5.



Scheme 5

The triplet at 1.794 ppm ( $\rho$ ), with a  $^3\text{J}_{\text{F,H}}$  of 19.5 Hz (Figure 1), is a singlet in the decoupled spectrum (Figure 2). Furthermore, the fluorine signal K at 107.415 ppm (Figure 4) is a quartet with the analogous  $^3\text{J}_{\text{F,H}}$  of 20.0 Hz (Table 3), giving the assignment to a  $-\text{CF}_2\text{-CH}_3$  end group. The  $^{19}\text{F}/^1\text{H}$  HETCOR (Figure 5) shows K to be coupled to  $\rho$  at 1.794 ppm but not to any other protons. Published data from unresolved spectra<sup>11, 12</sup> suggest this signal originates from a  $\text{CH}_3\text{-CF}_2\text{-CF}_2\text{-}$  end group; indeed in the  $^{19}\text{F}$  COSY (Figure 6) K does couple to L at  $-114.319$  ppm, which couples further to the main-chain proton signal  $\phi$  at 2.905 ppm giving the sub-structure  $\phi\text{-L-K-}\rho$  and all signals have commensurate relative intensities in the respective spectra. Thus K and L should give  $^3\text{J}_{\text{F,F}}$ . However, the signal K is a singlet when proton decoupling is applied whereas L is a broad triplet with an apparent  $\sim 10$  Hz  $^3\text{J}_{\text{F,F}}$  coupling. The coupling of L to K is questionable as the signal K, which has an 8

Hz linewidth, should also show the 10 Hz coupling seen in signal L and it does not. A possible explanation for this is that the  $^3J_{F,F}$  coupling of K to L is smaller than 8 Hz and the coupling of 10 Hz for L is  $^4J_{F,F}$ . This would be in agreement with the known attenuation of fluorine couplings<sup>19,39,40</sup>, suggesting the end-group structure shown in Scheme 6.



Scheme 6

### 5. Short-chain oligomers showing similar $^{19}\text{F}$ , $^{19}\text{F}$ coupling

Many of the  $^{19}\text{F}$  signals, such as H-T, F, G, and B, show increased resolution due to decoupling, but do not allow measurement of the magnitude of  $^3J_{F,F}$  or  $^4J_{F,F}$  because linewidths are 10 Hz or more. Along with signal C, these resonances are here assigned to fluorine groups adjacent to the defect units or end groups (see section 3). The signals C, H and I also show an increase in resolution due to decoupling. Although the signals H and I have been discussed in previous sections, the affect of decoupling on these signals is worth an special mention here. Both The signals H and I give a  $^4J_{F,F}$  of  $\sim 9.5$  Hz and C is resolved into two separate signals, now labelled C' and C (Figures 9a and b) at  $-94.577$  and  $-94.659$  ppm respectively. A  $^4J_{F,F}$  of 9.5 Hz for C' is also seen. Furthermore, new signals (N, O, and P) are observed in the region of the main-chain fluorine signal H-T at  $-91.897$  ppm, with a  $^3J_{F,F}$  of 9.5 Hz. The fluorine signals C', H and I (figure 9b) are all triplets with different integral values but have very similar  $^4J_{F,F}$  values of  $\sim 9.5$  Hz as do N, O and P. However credible integral values for N and O are not obtainable due to insufficient resolution, but the signal P has the same integral as H and they do couple in the  $^{19}\text{F}$  COSY spectrum as shown above. The proton-coupled fluorine spectra show the signals H and I with multiplet intensities 1:2:5:8:10:12:10:8:5:2:1, which could be from a four-spin system showing  $^4J_{F,F} \sim 9.5$  Hz and  $^3J_{F,H} \sim 19$  Hz.

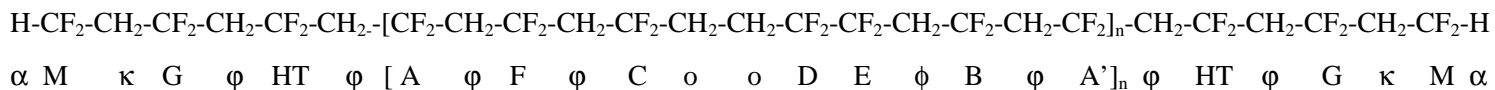
The  $^{19}\text{F}/^1\text{H}$  HETCOR spectrum (Figure 5 and Table 4) of the  $\text{CF}_2$  signal H shows coupling to the  $\text{CH}_2$  protons ( $\theta$ ) in the  $-\text{CH}_2-\text{CF}_2-\text{CH}_2-\text{CH}_3$  end group, so it is assigned as shown in Scheme 5. In the same spectrum signal H can be seen to couple to signal  $\omega$ . From the  $^{19}\text{F}$  COSY experiment (Figure 6) H is shown to couple to P. The signal H also shows coupling to protons of minor intensity ( $\omega$ ) and I to  $\varphi$ , though resolution does not allow a complete

assignment of the fluorine or proton signals No further coupling can be verified for P again due to resolution.

### 6. The main-chain structures

From the  $^{19}\text{F}$  and  $^1\text{H}$  correlation spectroscopy discussed in the previous sections, it is seen that the fluorines of the defect units (A' and F) scheme 3, both couple to the main-chain signal (H-T), which in turn couples to G of the end group, scheme 1 (see Figure 6). It is also important to note here the relative integral values of the end group protons and fluorine signals (G, M,  $\kappa$  and  $\alpha$ ) in scheme1, show relative integral values of 4, double that of the defect unit signals and adjacent groups. This true for integral values presented in both the proton and fluorine data, tables 1 and 2 (compare  $\alpha$  with  $\phi$  and M and G with D or E respectively). Furthermore, no other signal with corresponding integral values or correlation, was found to be associated with these groups.

On the basis of these observations a tentative structural type (Scheme 7) for the main component in the reaction mixture can be suggested were the end groups are the same.



Scheme 7

### 7. Degree of polymerisation and the reverse unit.

The degree of polymerisation ( $\overline{DP}_{ncum}$ ) and reverse unit (RU%) formation are commonly reported parameters for VDF polymers and are calculated by Equations (1) and (2)<sup>10</sup>:

$$\overline{DP}_{ncum} = \frac{HT + A + B + C + F + G + E + D}{M} \quad (1)$$

$$RU\% = \frac{E}{HT + A + B + C + F + G + M + E + D} \quad (2)$$

We calculate these parameters using the proton-coupled and -decoupled fluorine spectra with integration as follows:

The average cumulative degree of polymerisation was evaluated by integration of the fluorine signals representative of the VDF backbone, as indicated in Scheme 7 (H-T, A, B, C D, E, F, G) and the fluorine signal M representing the end groups. Using integrated values of signals from the  $^1\text{H}$ -decoupled  $^{19}\text{F}$  NMR (Table 3) and equation 1 the degree of polymerisation is estimated to be 18 and, using a molecular weight of 64 for the  $(-\text{CH}_2-\text{CF}_2-)$  unit, an average molecular weight for the VDF telomer was found to be 1200 Dalton. The decoupled spectrum should give a more accurate assessment of these parameters than the coupled spectrum. However, in the literature proton spectra without decoupling are often used. Moreover, the main-chain signal often has contributions from signals not associated with the polymer backbone structure, leading to possibly erroneous evaluations.

A reverse-unit content was calculated to 3%, using Equation 2 with integral values from the proton-decoupled fluorine spectrum. As stated earlier, the amount of reverse units is usually large in the early stages of polymerisation, up to 50%, and decreases with increase in molecular weight<sup>34</sup>. In this study, the amount of reverse units is low and comparable to values reported for photochemically induced polymerisation<sup>10</sup>. The reverse-unit values measured from the fluorine spectra for our low molecular weight VDFT (1200 D) is about half of that for PVDF ( $1 \times 10^6$  D)<sup>10, 34</sup>.

## CONCLUSIONS

The decoupling of  $^{19}\text{F}$  or  $^1\text{H}$  when  $^1\text{H}$  or  $^{19}\text{F}$  spectra are being acquired, respectively, results in a significant improvement in resolution, clearly seen in the  $^{19}\text{F}$  spectra for the VDFT  $^{19}\text{F}$  signals N, O, P H, I and C', which are to our knowledge not previously assigned in the literature on VDFT. Decoupling has also allowed verification of  $^3\text{J}_{\text{F,H}}$  and  $^4\text{J}_{\text{F,H}}$  coupling constants, which were found to be in general agreement with literature values. Two structures are tentatively presented, one with reverse units scheme 7, and one apparently without, scheme 2. As the linewidths for the higher molecular weight compound, scheme 7, showed typical values in excess of 10 Hz, splittings arising from  $^4\text{J}_{\text{F,F}}$  ( $\sim 9.5$  Hz) were only resolved for the compound with no reverse units i.e. lower molecular weight. We suggest this compound has a lower value of  $\overline{DP}_{cum}$ , though this could not be calculated, because of the limited spectral resolution. We also conclude that the proton-decoupled fluorine spectra should give more accurate values for reverse unit and end group content due to higher

resolution of the signals in question. The increased resolution available from decoupling also aided the determination of new hetero- and homo-nuclear coupling constants. It was found that  ${}^3J_{F,F}$  can be greater than  ${}^4J_{F,F}$ , as in the case for the reverse-unit signals, and vice versa. This shows that great care must be taken in the structural determination of highly fluorinated compounds. The fluorine spectrum of VDFT shows signals of specific interest, namely J and K. We have assigned these signals to small molecular by-products.. Although several end-group signals appear in the spectra of VDFT, only the  $CF_2H$  end group was shown to terminate the main polymer chain based on correlation and integral values. Signals associated with major polymer backbone structures have linewidths, which are generally equal to or greater than the magnitude of homonuclear  ${}^3J_{F,F}$  and  ${}^3J_{H,H}$  coupling constants, making their determination difficult. This work has shown that the main reaction product has reactive end groups giving the possibility of further modification and aided our understanding of the structural complications of these compounds.

## REFERENCES

- 8
- 9
- 10
- 11 **1** Ferguson RC. *J. Am. Chem. Soc.*, 1960; 82: 2416.
- 12
- 13 **2** Gorlitz M, Minke R, Trautvet W, Weisgerb G. *Angewandte Makromol. Chemie*, 1973; 29-3: 137.
- 14
- 15 **3** Ferguson RC, Ovenall DW. *Abstracts of Papers of the American Chemical Society*, 1984; 187: 157.
- 16
- 17 **4** Macheteau JP, Oulyadi H, van Hemelryck B, Bourdonneau M, Davoust D. *J. Fluorine Chem.*, 2000;  
18 **104: 149.**
- 19
- 20 **5** Battiste J, Newmark RA. *Prog. NMR Spectr.*, 2006; 48: 1.
- 21
- 22 **6** Battiste JL, Jing NY, Newmark PA. *J. Fluorine Chem.*, 2004; 125: 1331.
- 23
- 24 **7** Boyer C, Valade D, Lacroix-Desmazes P, Ameduri B, Boutevin B. *J. Polym. Sci. Part a-Polym. Chem.*,  
25 **2006; 44: 5763.**
- 26
- 27 **8** Guiot J, Ameduri B, Boutevin B, Lannuzel T. *European Polym. J.*, 2003; 39: 887.
- 28
- 29 **9** Mladenov G, Ameduri B, Kostov G, Mateva R. *J. Polym. Sci. Part a-Polym. Chem.*, 2006; 44: 1470.
- 30
- 31 **10** Saint-Loup R, Ameduri B. *J. Fluorine Chem.*, 2002; 116: 27.
- 32
- 33 **11** Pianca M, Barchiesi E, Esposito G, Radice S. *J. Fluorine Chem.*, 1999; 95: 71.
- 34
- 35 **12** Russo S, Behari K, Chengji S, Pianca M, Barchiesi E, Moggi G. *Polymer*, 1993; 34: 4777.
- 36
- 37 **13** Herman, Uno T, Kubono A, Umemoto S, Kikutani T, Okui N. *Polymer*, 1997; 38: 1677.
- 38
- 39 **14** Katoh E, Ogura K, Ando I. *Polym. J.*, 1994; 26: 1352.
- 40
- 41 **15** Kharroubi M, Manseri A, Ameduri B, Boutevin B. *J. Fluorine Chem.*, 2000; 103: 145.
- 42
- 43 **16** Manseri A, Ameduri B, Boutevin B, Chambers RD, Caporiccio G, Wright AP. *J. Fluorine Chem.*,  
44 **1995; 74: 59.**
- 45
- 46 **17** Ameduri B, Duc M, Kharroubi M, Boutevin B. *Abstracts of Papers of the American Chemical Society*,  
47 **1998; 216: U90.**
- 48
- 49 **18** Ameduri B, Boutevin B, Kostov GK, Petrova P. *Des Monomers Polym*, 1999; 2: 267.
- 50
- 51 **19** Newmark RA, Graves RE. *J. Chem. Phys.*, 1967; 47: 3681–3682.

- 52  
53 **20** Raulet R, Grandclaude D, Humbert F, Canet D. *J Magn Reson*, 1997; 124: 259.  
54  
55 **21** Jones BG, Branch SK, Threadgill MD, Wilman DEV. *J. Fluorine Chem.*, 1995; 74: 221.  
56  
57 **22** Bailey WI, Kotz AL, McDaniel PL, Parees DM, Schweighardt FK, Yue HJ, Anklin C. *Anal. Chem.*,  
58 **1993; 65: 752.**  
59  
60 **23** Bruch MD, Bovey FA, Cais RE. *Macromolecules*, 1984; 17: 2547–2551.  
61  
62 **24** Cais RE, Kometani JM. *Macromolecules*, 1985; 18: 1354–1357.  
63  
64 **25** Wormald P, Apperley DC, Beaume F, Harris RK. *Polymer*, 2003; 44: 643.  
65  
66 **26** Yu H, J. M, Ni. H, J. C. *J. Microwave Radiofreq. Spectr.*, 1984; 1: 372.  
67  
68 **27** Muracheva YM, Shashkov AS, Dontsov AA. *Polym. Sci. USSR*, 1981; 23: 711.  
69  
70 **28** Kostov G, Ameduri B, Boutevin B. *J. Fluorine Chem.*, 2002; 114: 171.  
71  
72 **29** Souzy R, Ameduri B. *Prog. Polym. Sci.*, 2005; 30: 644.  
73  
74 **30** Wormald P, Ameduri B, Harris RK, Hazendonk P. *Solid State NMR*, 2006; 30: 114.  
75  
76 **31** Hazendonk P, Harris RK, Ando S, Avasse P. *J Magn Reson*, 2003; 162: 206.  
77  
78 **32** Ando S, Harris RK, Hazendonk P, Wormald P. *Macromol. Rapid Comm.*, 2005; 26: 345.  
79  
80 **33** Ando S, Harris RK, Reinsberg SA. *Magn. Reson. Chem.*, 2002; 40: 97.  
81  
82 **34** Duc M, Ameduri B, Boutevin B, Kharroubi M, Sage J-M. *Macromol. Chem. Phys.*, 1998; 199: 1271.  
83  
84 **35** Diehl P, Harris RK, Jones RG. *Prog. NMR Spectry.*, 1967; 3: 1.  
85  
86 **36** Ameduri B, Boutevin B, Fruchier A, Kostov GK, Petrova P. *J. Fluorine Chem.*, 1998; 89: 167.  
87  
88 **37** Sauguet L, Boyer C, Ameduri B, Boutevin B. *Macromolecules*, 2006; 39: 9087.  
89  
90 **38** Schwarz R, Seelig J, Kunnecke B. *Magn. Reson. Chem.*, 2004; 42: 512–517.  
91  
92 **39** Abraham RJ, Cavalli L. *Mol. Phys.*, 1965; 9: 67–75.  
93  
94 **40** Berger S, Braun S, Kalinowski H-O, *NMR Spectroscopy of the Non-*  
95 *Metallic Elements*, Wiley, New York, 1997.  
96

Figure 1

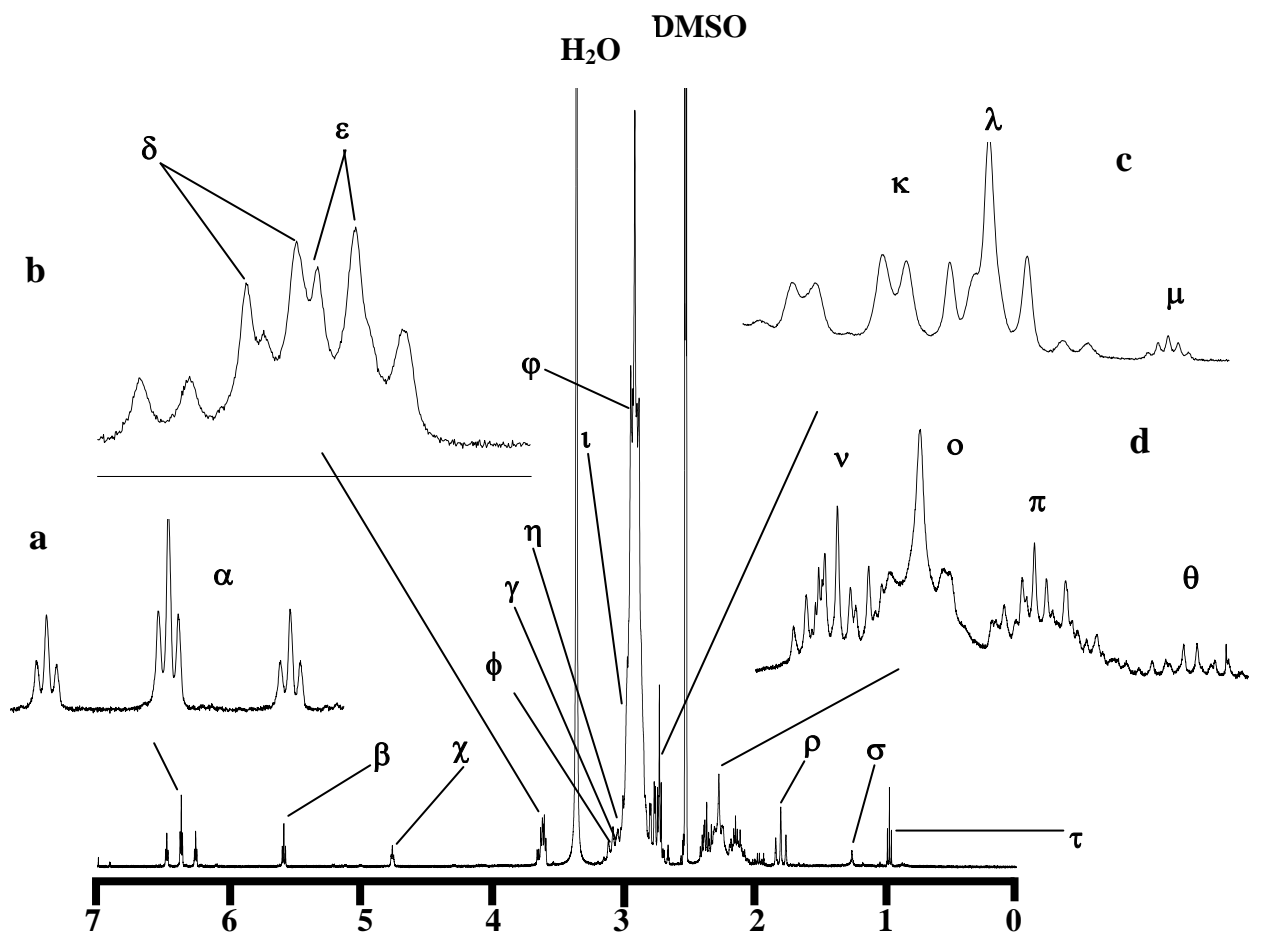
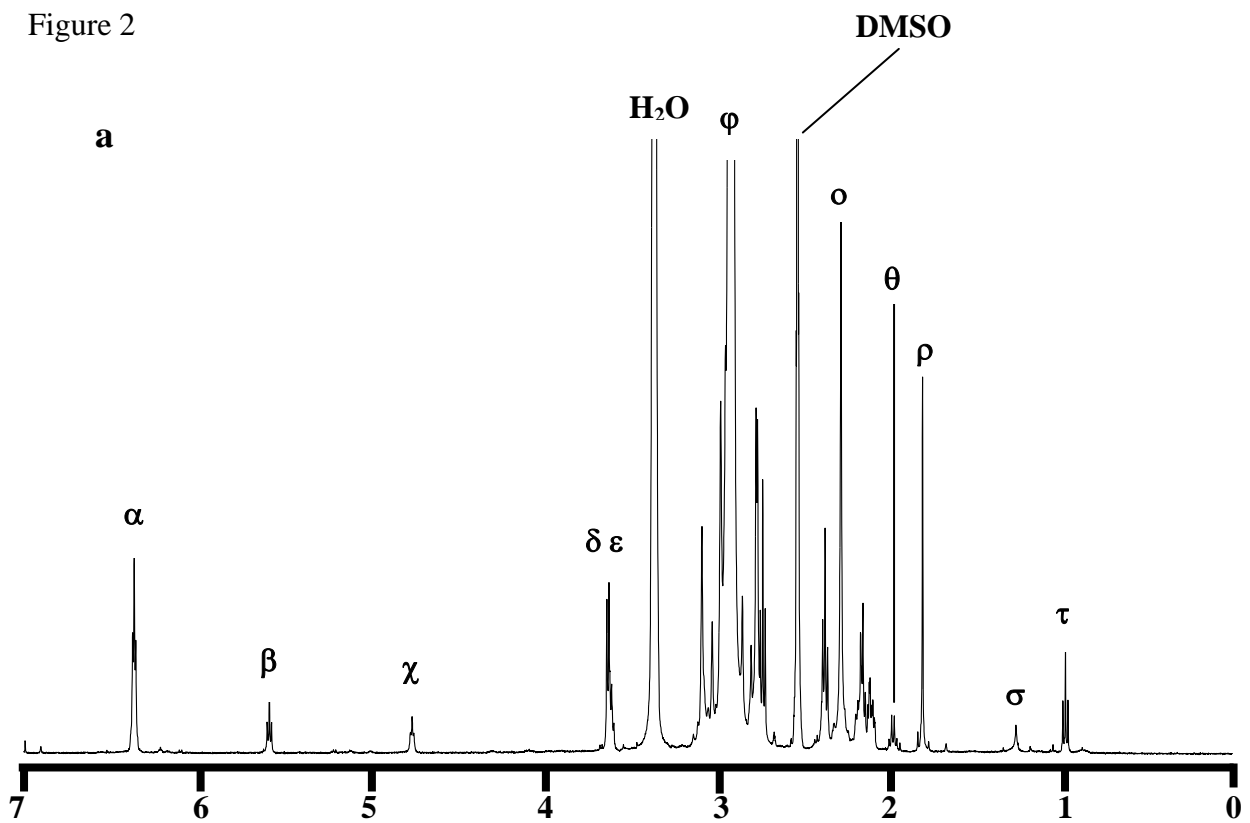


Figure 2



b

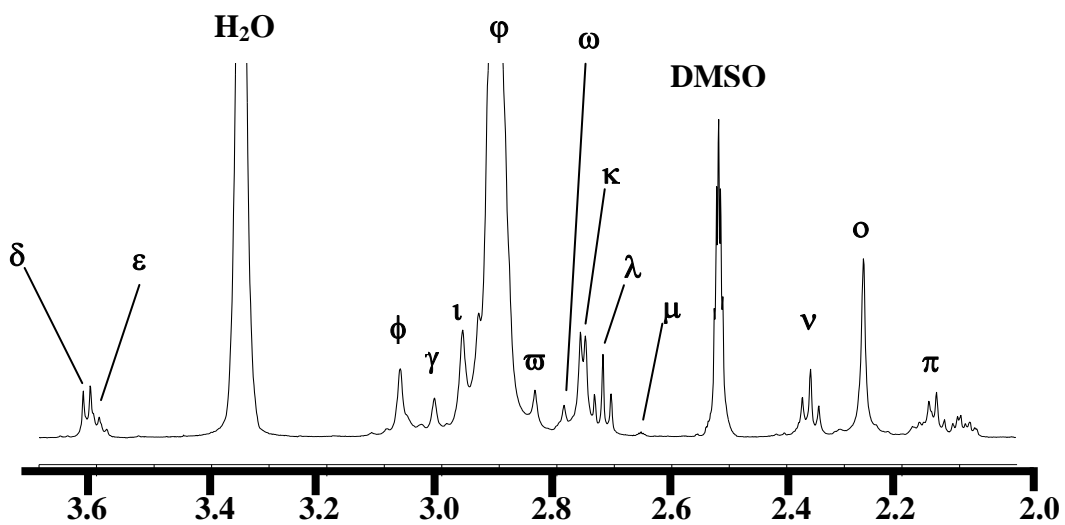
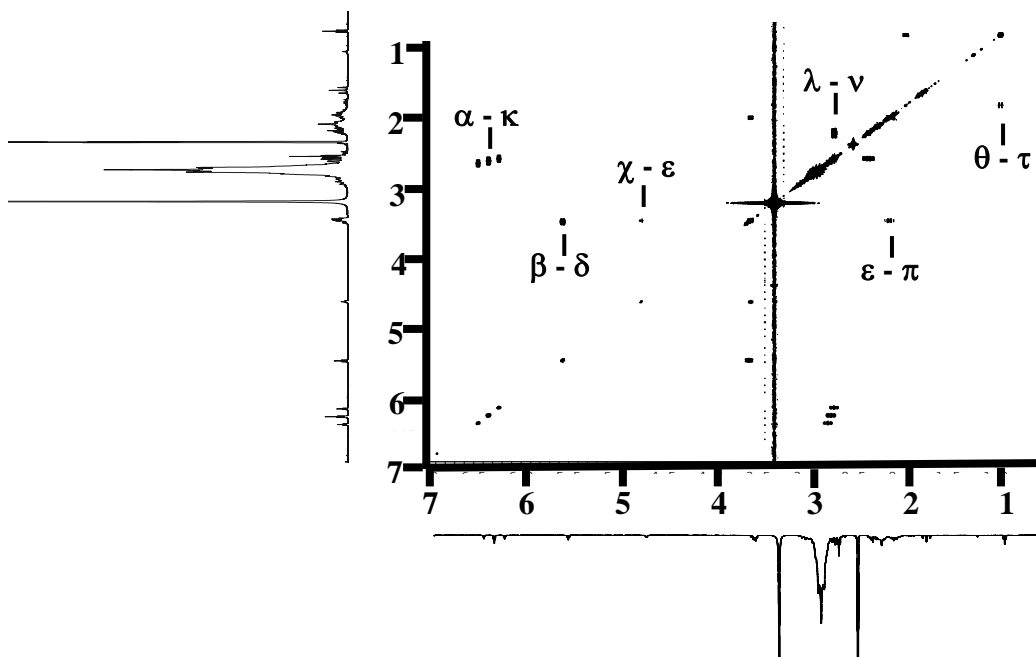
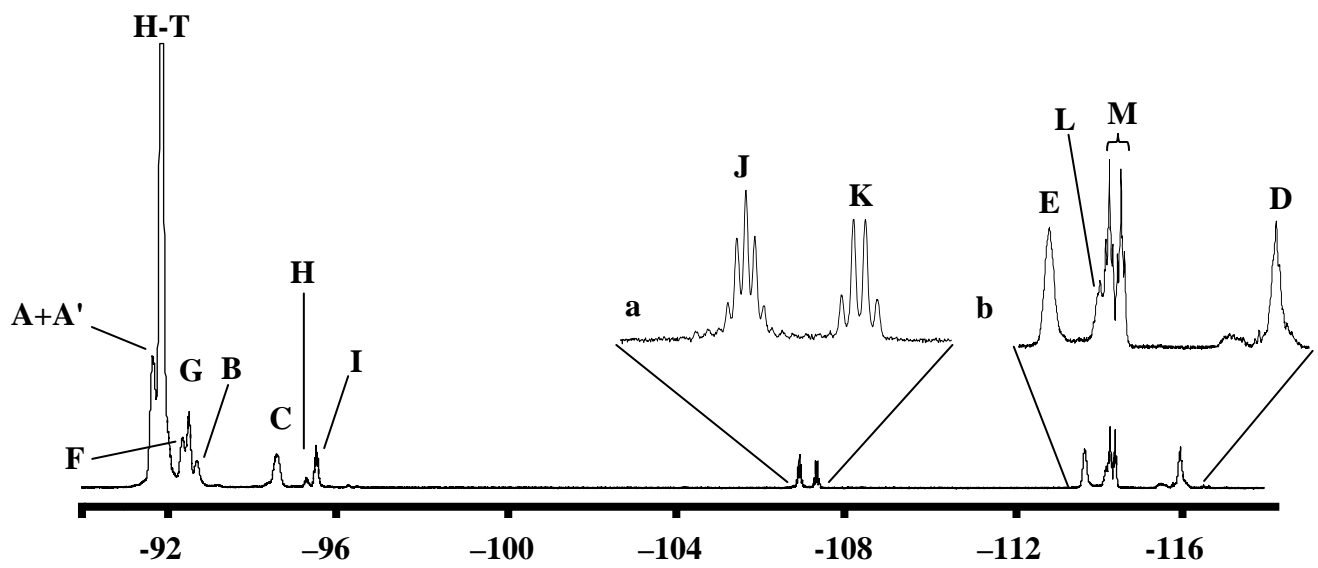


Figure 3



a

Figure 4



b

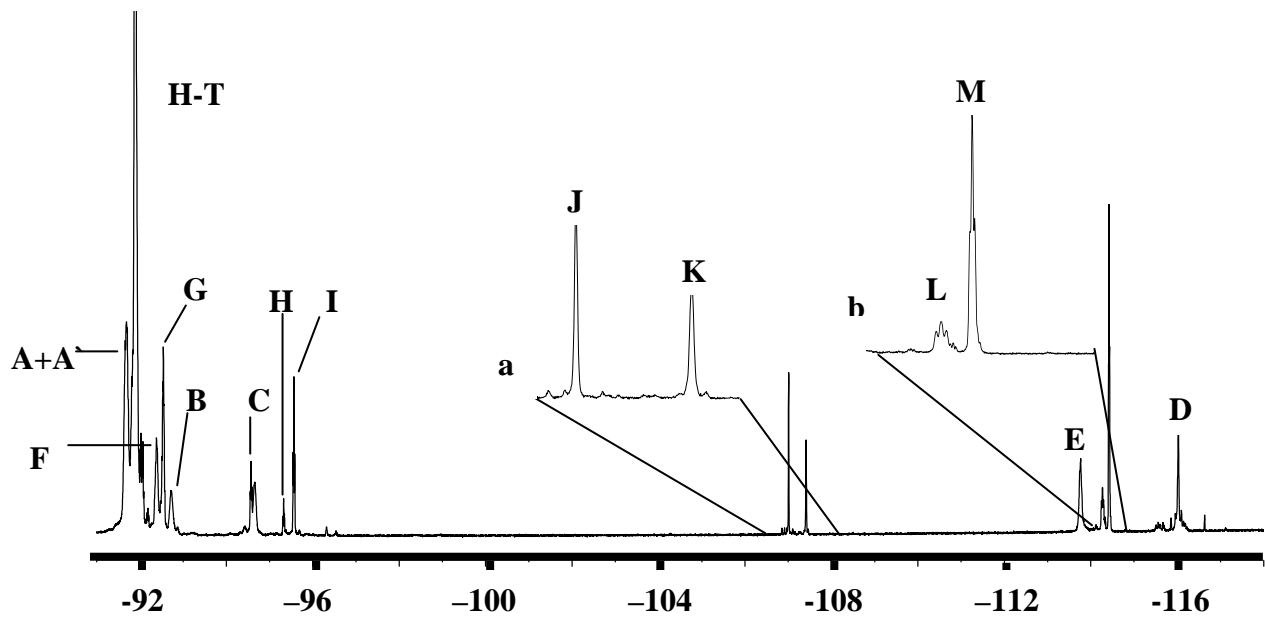


Figure 5

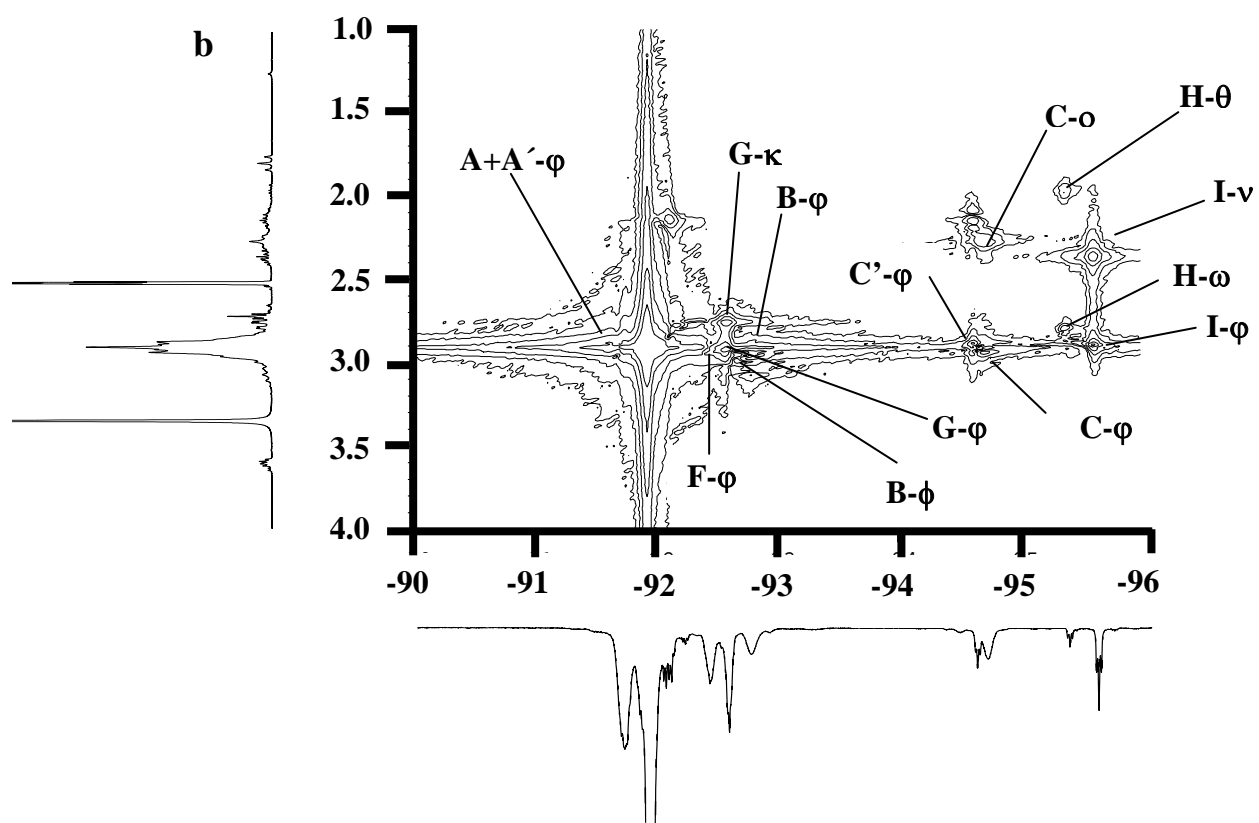
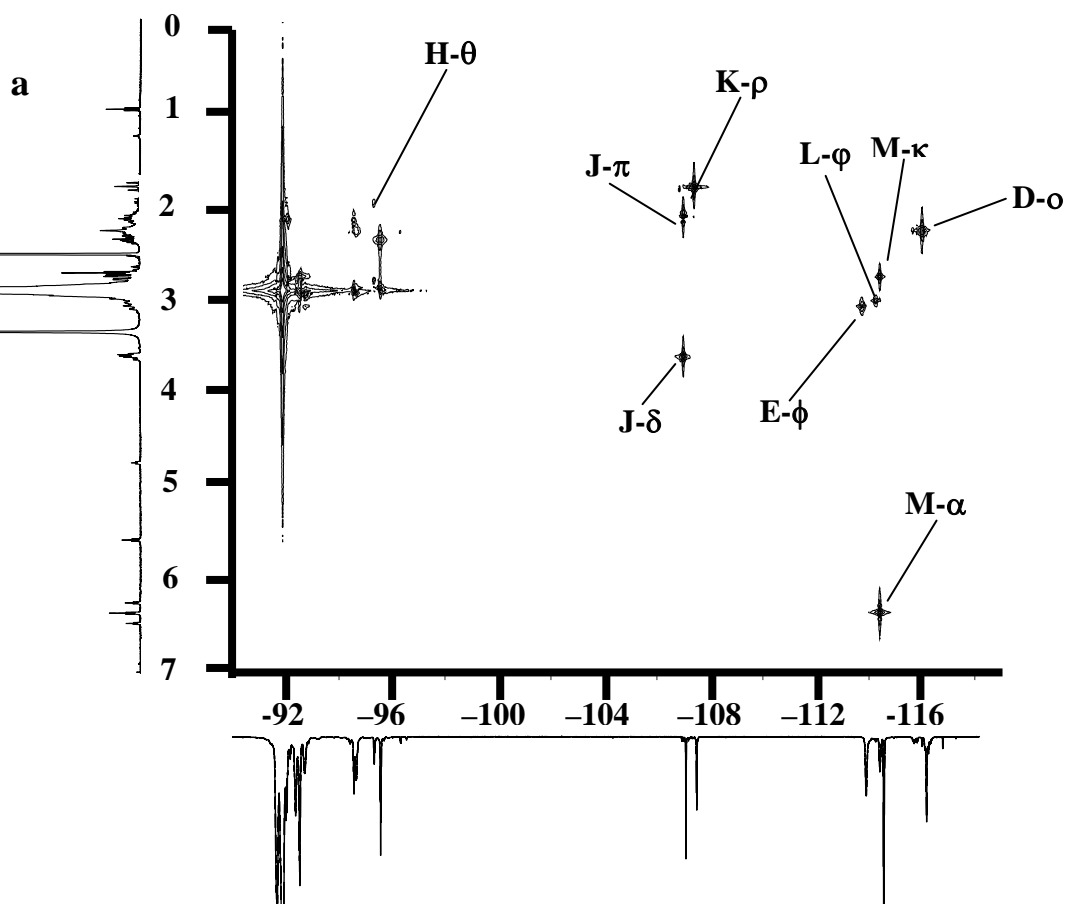
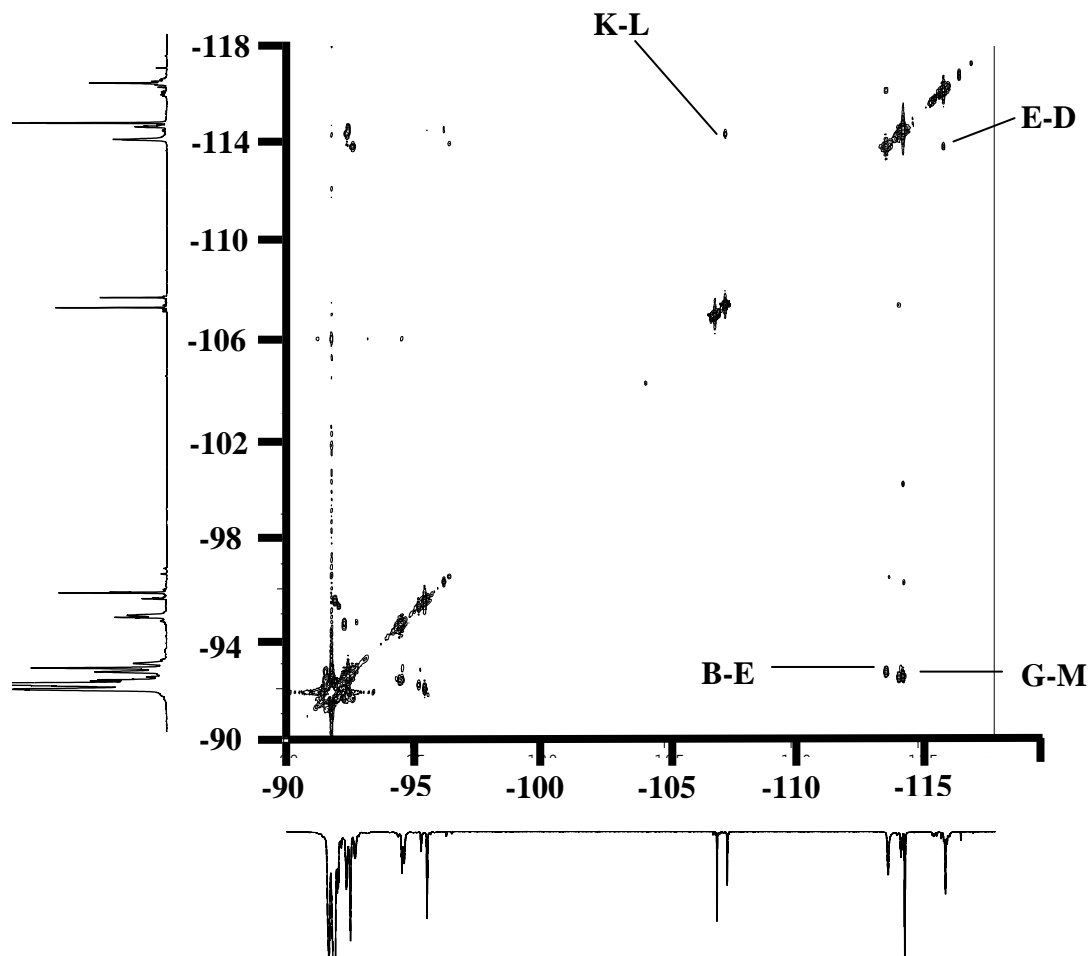


Figure 6

**a**



**b**

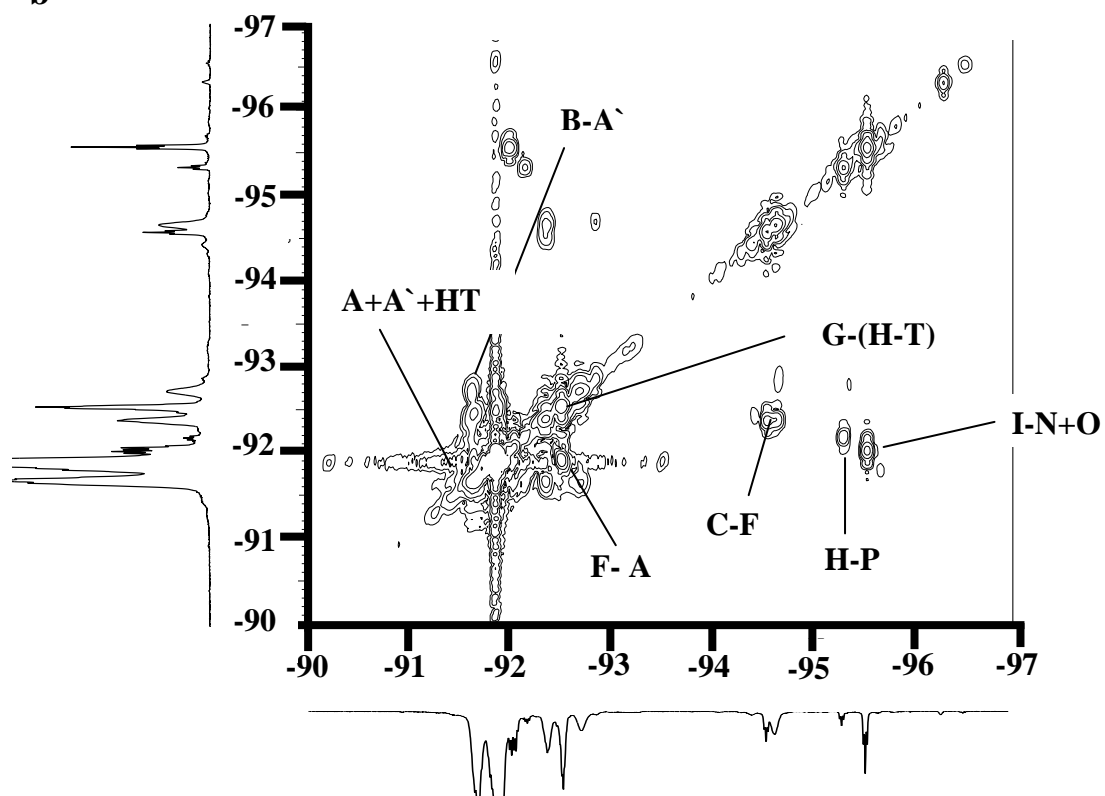


Figure 7

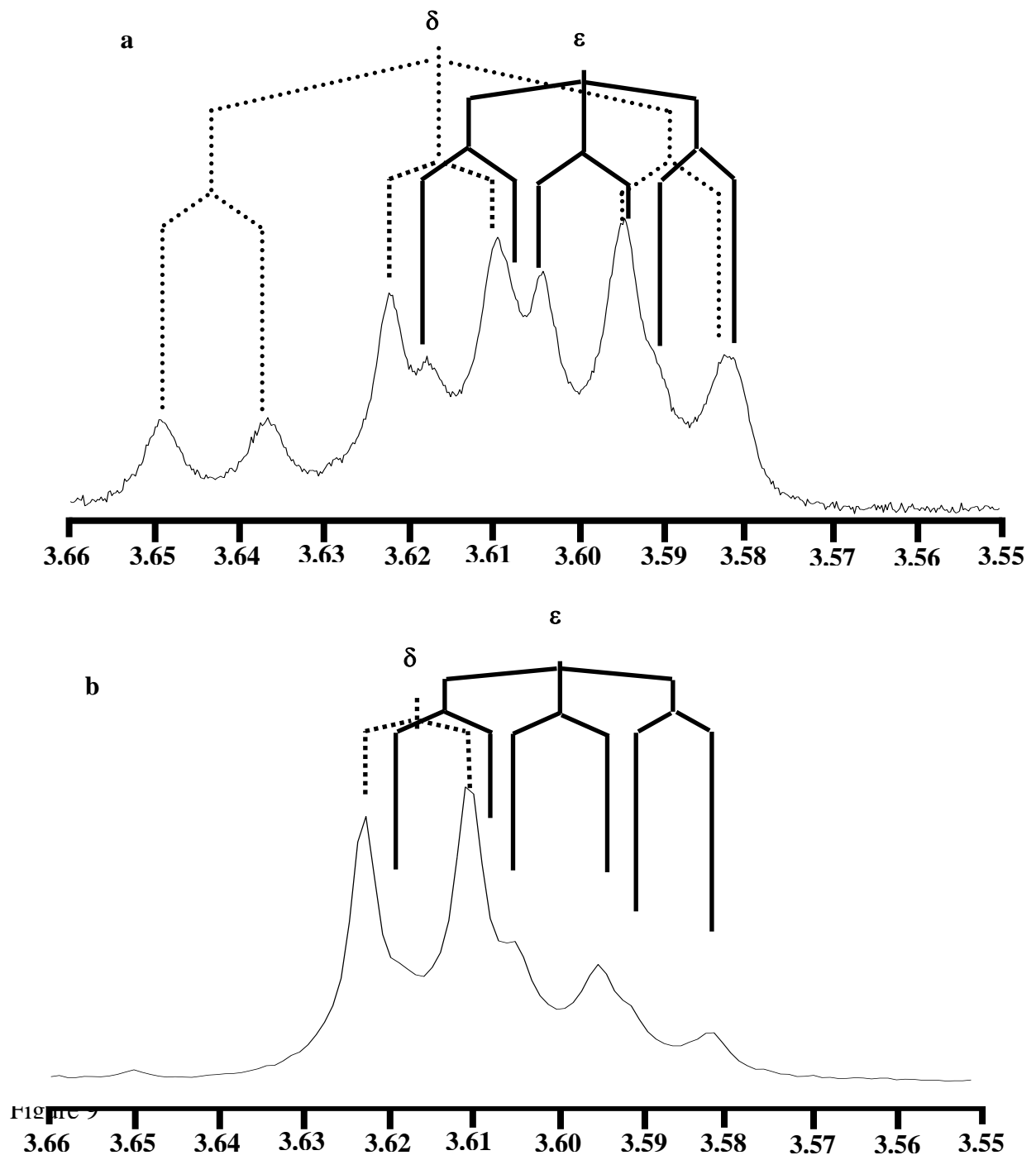


Figure 8

